

# On the Heating Efficiency Derived from Observations of Young Super Star Clusters in M82

Sergiy Silich<sup>1</sup>, Guillermo Tenorio-Tagle<sup>1</sup>, Ana Torres Campos<sup>1</sup>,

Casiana Muñoz-Tuñón<sup>2</sup>, Ana Monreal-Ibero<sup>2,3</sup>, Veronica Melo<sup>2</sup>

## ABSTRACT

Here we discuss the mechanical feedback that massive stellar clusters provide to the interstellar medium of their host galaxy. We apply an analytic theory developed in a previous study for M82-A1 to a sample of 10 clusters located in the central zone of the starburst galaxy M82, all surrounded by compact and dense HII regions. We claim that the only way that such HII regions can survive around the selected clusters, is if they are embedded into a high pressure ISM and if the majority of their mechanical energy is lost within the star cluster volume via strong radiative cooling. The latter implies that these clusters have a low heating efficiency,  $\eta$ , and evolve in the bimodal hydrodynamic regime. In this regime the shock-heated plasma in the central zones of a cluster becomes thermally unstable, loses its pressure and is accumulated there, whereas the matter injected by supernovae and stellar winds outside of this volume forms a high velocity outflow - the star cluster wind. We calculated the heating efficiency for each of the selected clusters and found that in all cases it does not exceed 10%. Such low heating efficiency values imply a low mechanical energy output and the impact that the selected clusters provide to the ISM of M82 is thus much smaller than what one would expect using stellar cluster synthetic models.

*Subject headings:* galaxies: individual (M82) — galaxies: star clusters — HII regions — ISM: bubbles — kinematics and dynamics

## 1. Introduction

It is a common believe that massive star clusters return a significant fraction of their stellar mass to the interstellar medium (ISM). This is thought to be done in a violent manner

---

<sup>1</sup>Instituto Nacional de Astrofísica Óptica y Electrónica, AP 51, 72000 Puebla, México; silich@inaoep.mx

<sup>2</sup>Instituto de Astrofísica de Canarias, E 38200 La Laguna, Tenerife, Spain; cmt@ll.iac.es

<sup>3</sup>European Southern Observatory, Karl-Schwarzschild-Strasse 2 D-85748 Garching bei München, Germany

that deeply affects the structure of the interstellar gas and in the case of starburst galaxies, this may even result in the channeling of the processed material into the intergalactic space (see, for instance, Tenorio-Tagle et al. 2003, Cooper et al. 2008, and references therein). The general consensus is that within the volume occupied by superstar clusters (SSCs), the kinetic energy supplied by massive stars in the form of stellar winds and supernovae explosions is there in situ thermalized. This results into a high temperature ( $T \sim 10^7\text{K}$ ) plasma, with a large thermal pressure that highly exceeds that in the ambient ISM, and this provokes the exit of the thermalized ejecta out of the cluster as a supersonic star cluster wind (Chevalier & Clegg, 1985). The cluster winds shape the ISM by generating large-scale superbubbles. These shock and displace the surrounding ISM while locking it into large expanding shells able to cool down by radiation in a short characteristic time scale, while the much lower density shock-heated wind gas, which fills the superbubble interior, remains hot for a considerably longer time (Weaver et al. 1977; Mac Low & McCray, 1988; Tenorio-Tagle et al. 2006) and promotes the growth of the superbubble. This shocked wind plasma has been detected around OB-associations and stellar clusters as a soft X-ray emitter (see, for example, Chu et al. 1995; Stevens & Hatwell 2003, Silich et al. 2005 and references therein), whereas the outer shells have been traced in 21 cm (Puche et al. 1992, Ehlerová et al. 2004) or as photoionized engulfing filaments, if in presence of a strong Lyman continuum radiation (Meaburn, 1980; Lozinskaya, 1992 and references therein). The size and interior pressure of superbubbles in the case of an homogeneous interstellar gas distribution (see Mac Low & McCray, 1988; Bisnovatyi-Kogan & Silich 1995 and references therein) are:

$$R_{sb} = \left( \frac{375(\gamma - 1)}{28(9\gamma - 4)\pi} \right)^{1/5} \left( \frac{L_{out}}{\rho_{ISM}} \right)^{1/5} t^{3/5}, \quad (1)$$

$$P_{sb} = 7\rho_{ISM} \left[ \frac{3(\gamma - 1)}{700(9\gamma - 4)\pi} \frac{L_{out}}{\rho_{ISM}} \right]^{2/5} t^{-4/5}, \quad (2)$$

where  $\gamma = 5/3$  is the ratio of specific heats,  $R_{sb}$  is the outer shell radius,  $P_{sb}$  is the pressure in the shock-heated wind region,  $L_{out}$  is the star cluster mechanical energy output,  $\rho_{ISM}$  is the interstellar gas density, and  $t$  the evolutionary time. The superbubbles are supposed to expand until they acquire pressure equilibrium with the surrounding medium ( $P_{sb} = P_{ISM}$ ), when:

$$R_{sb} = (7\gamma)^{3/4} \left[ \frac{3(\gamma - 1)}{28(9\gamma - 4)\pi} \frac{L_{out}}{\rho_{ISM} a_{ISM}^3} \right]^{1/2} = 637 \left( \frac{L_{38}}{n_{ISM} a_{10}^3} \right)^{1/2} pc, \quad (3)$$

where  $n_{ISM}$  is the interstellar gas number density,  $L_{38}$  is the mechanical energy output in units of  $10^{38}$  erg s $^{-1}$  and  $a_{10}$  is the sound speed in the interstellar medium in units of 10 km s $^{-1}$ .

However, as noticed by Silich et al. (2007), this cannot be the whole story. The observed

properties of the HII region associated to the massive ( $1.3 \times 10^6 M_{\odot}$ ), young (age  $\sim 6$  Myr) and thus powerful (with a mechanical luminosity,  $L_{mech} \approx 2.5 \times 10^{40}$  erg s $^{-1}$ ) super star cluster M82-A1 (Smith et al. 2006) are not consistent with the interstellar bubble model (equations 1 - 3). The associated minute, low mass ( $M_{HII} \approx 5 \times 10^3 M_{\odot}$ ), although dense ( $n_{HII} \approx 1800$  cm $^{-3}$ ), HII region presents a radius ( $R_{HII} \approx 4.5$  pc) much smaller than that predicted by equations (1 and 3). It seems surprising that M82-A1 and other young and massive clusters in M82 (Melo et al. 2005), NGC 3351 (Hägele et al. 2007) and in other galaxies are surrounded by compact, low mass (see Table 2 below) HII regions despite the powerful mechanical energy output predicted for the clusters by stellar evolution synthesis models.

Silich et al. (2007) suggested that in this case clearly only a fraction of the star cluster mechanical luminosity is converted into the energy of the outflowing plasma whereas the rest ought to be lost due to strong radiative cooling. They also developed an analytic and semi-analytic model, which led to obtain the value of the heating efficiency  $\eta$ , the parameter which links the star cluster mechanical luminosity with the actual thermal energy that is deposited into the star cluster volume. The models reveal the value of the heating efficiency by fitting the ionized gas number density and radius of the compact HII region detected around a massive star cluster. The results led to a low heating efficiency ( $\eta < 10\%$ ) in the case of M82-A1.

Here we extend the analysis of Silich et al. (2007) to a sample of 10 SSCs selected from the list of Melo et al. (2005), in order to reveal their heating efficiency, and thus the energy that these clusters return to the ISM of M82.

Section 2 and 3 discuss the hydrodynamics of SSCs, the model assumptions and present the equations used in order to obtain the heating efficiency. The sample of the selected clusters is presented in section 4. We apply our model to each of the selected clusters and discuss our results in section 5.

## 2. The heating efficiency in SSCs

The hydrodynamics of the matter returned by stellar winds and supernova explosions within the cluster volume has been approximated assuming first that the sources are equally spaced within a spherical volume of radius  $R_{SC}$ . In the pioneer adiabatic approach of Chevalier & Clegg (1985), the kinetic energy supplied by the evolving massive stars,  $L_{mech}$ , has been assumed to be completely converted into thermal energy of the hot plasma. The strong pressure gradient generated by the deposited matter, forces then the gas velocity to increase

almost linearly from  $0 \text{ km s}^{-1}$  at the star cluster center to its sound speed at the cluster edge. Once the gas streams out of the cluster, it rapidly acquires its terminal speed ( $v_{A\infty} \sim 2c_{SC}$ ), while its density and temperature drop as  $r^{-2}$ , and  $r^{-4/3}$ , respectively.

More recently, Silich et al. (2004), Tenorio-Tagle et al. (2005, 2007) and Wünsch et al. (2008) recognized that the adiabatic assumption is not valid in the case of massive and compact star clusters and developed a radiative star cluster wind model, which takes into consideration the energy losses that occur in the hot thermalized plasma. They found a threshold line,  $L_{crit}(R_{SC})$  in the  $L_{mech} - R_{SC}$  parameter space. The radiative solution is in excellent agreement with Chevalier & Clegg’s results in the case of low mass clusters, when  $L_{mech} \ll L_{crit}$ . However, strong radiative cooling modifies essentially the temperature distribution outside of the cluster when the star cluster mechanical luminosity approaches the threshold value,  $L_{mech} \leq L_{crit}$ . When the mechanical luminosity of the considered clusters exceeds the threshold value,  $L_{crit}$ , catastrophic cooling sets in within the central zones of the cluster, what results into a bimodal flow regime. In this case the stagnation radius,  $R_{st}$ , moves out of the cluster center and splits the cluster volume into two distinct zones. In the inner zone,  $r < R_{st}$ , strong radiative cooling promotes frequent thermal instabilities in the injected gas, reducing significantly the pressure gradient and thus the outward acceleration. Strong radiative cooling thus leads to the accumulation of the matter injected within the volume defined by the stagnation surface. In the outer zone,  $R_{st} < r < R_{SC}$ , despite radiative cooling, the pressure gradient remains sufficient to drive the injected matter away from the cluster, as a strongly radiative stationary wind.

The detail physics during the thermalization process are however not well understood. In the original paper of Chevalier & Clegg (1985) it was assumed that the amount of the deposited thermal energy per unit volume,  $q_e$ , is identical to the rate of mechanical energy released by massive stars:  $q_e = q_{mech}$ . However Stevens & Hartwell (2003) found that this assumption is not in good agreement with the spectra of the diffuse X-ray emission detected in a number of nearby massive clusters. Bradamante et al. (1998), and Recchi et al. (2001), who studied the chemical and dynamical evolution of blue compact galaxies, also claimed that only a few per cent of the energy deposited by supernovae type II provides the energetics of the host galaxy ISM, while the rest is radiated away. It is therefore highly desirable to link the value of the heating efficiency with stellar clusters observable quantities.

A firm evidence for an incomplete transformation of the star cluster mechanical luminosity into the energy of the star cluster wind was obtained by Smith et al. (2006), who provided detailed photometric and spectral analysis of the massive, young SSC M82-A1 and its associated HII region. This led them, as well as to Silich et al. (2007), to claim that the energy  $q_e$  represents only a small fraction of the mechanical energy provided by massive

stars:  $q_e = \eta q_{mech}$ , with  $\eta \ll 1$ . The physical justification for this parameter comes from the fact that strong radiative cooling may take place during the process of thermalization either because of an enhanced gas metallicity, resultant from SN explosions, or because of the large densities within the shock-heated zones between neighboring massive stars, before the newly injected matter joins the flow (Wünsch et al. 2007; Silich et al. 2007). In this case only a fraction of the mechanical energy supplied by the collection of massive stars is shared by the matter within the cluster volume and thus the actual thermal energy given to the injected gas is smaller than that provided by the collection of massive stars. This is particularly important in the case of massive ( $M_{SC} \geq 10^5 M_\odot$ ) and compact ( $R_{SC} \sim$  a few parsecs) clusters which present a large massive star number density,  $N_\star$ , and a small mean separation between them:  $\Delta R = N_\star^{-3} \ll 1$  pc.

Indeed, the multiple interactions expected between supersonic stellar winds and the supernovae ejecta in such compact and massive clusters are similar to those occurring in colliding wind binaries that lead to a shock-heated plasma, that effectively radiates in the soft X-ray regime. Luo et al. (1990); Stevens et al. (1992) found that in the case of colliding wind binaries the amount of energy radiated away from the shock-heated zone,  $L_{lost}$ , depends on the binary separation. It scales as  $L_{lost} \sim \Delta R^{-1}$  in the quasi-adiabatic regime and increases when radiative cooling in the shock-heated zone is taken into consideration. In the case of a dense stellar cluster the kinetic energy placed by massive stars interacts with that deposited by multiple nearby neighbors. This suggests that the energy, which actually drives the star cluster outflow, is smaller than the total provided by the massive stars within the cluster volume, particularly if one accounts for the large metallicities expected from supernovae.

In the semi-analytic models all uncertainties dealing with the distribution of massive stars and the collisions between nearby supersonic flows and thus the sudden loss of energy, are accounted for by the parameter  $\eta$ , known as the heating efficiency. The fraction of energy that a star cluster returns to the ambient interstellar gas strongly depends on this parameter. Thus  $\eta$  defines the mechanical feedback that star clusters provide to the ISM of their host galaxy.

### 3. The pressure confined wind model

The pressure confined wind model (Silich et al. 2007) suggests that the combination of two factors is crucial in order to produce the compact and dense HII regions able to survive around powerful young clusters. These are a low heating efficiency and a large thermal pressure,  $P_{ISM}$ , in the surrounding ISM, what leads to a pressure confined bubble configuration. Thus in this model the size of the standing HII region depends critically

on the balance between  $P_{ISM}$  and the wind ram pressure at the reverse shock position ( $P_{ram} = P_{ISM}$ ). In this case the structure of the outflow can be derived analytically from a set of equations that consider: conservation of mass, photoionization balance, pressure equilibrium and the fast radiative cooling that occurs within the star cluster volume and on its wind. Our set of equations is such that if the parameters of the driving stellar cluster: its mass ( $M_{SC}$ ), radius ( $R_{SC}$ ), the number of ionizing photons ( $N^{SC}$ ) are known, one can match the model predicted radius ( $R_{HII}$ ) and gas number density ( $n_{HII}$ ) of the associated HII region with the observed values. In this approach, one can find the value of the heating efficiency from a nonlinear algebraic equation which relates  $\eta$  with the host cluster and the associated HII region parameters (see Silich et al. 2007):

$$1 - \frac{(4\pi P_{ISM} V_{A\infty}^2 R_{HII}^2)^{1/2}}{(4L_{crit} L_{SC} V_{\infty}^2)^{1/4}} \left[ \left( 1 - \frac{3f_t N^{SC}}{4\pi\beta n_{HII}^2 R_{HII}^3} \right)^{1/3} - \frac{9}{512} \frac{f_{\lambda} \mu_i^2 V_{\infty}^5}{P_{ISM} R_{HII} \Lambda_s} \right] = 0, \quad (4)$$

where  $V_{A\infty} = (2L_{SC}/\dot{M}_{SC})^{1/2}$  is the adiabatic wind terminal speed,  $L_{SC}$  and  $\dot{M}_{SC}$  are the star cluster mechanical luminosity and the mass input rate, respectively,  $\Lambda_s$  is the value of the cooling function at the reverse shock radius,  $\beta$  is the recombination coefficient to all but the ground level,  $f_{\lambda} = 0.3$  is a fiducial coefficient and  $f_t$  is the fraction of ionizing photons, which reaches the outer standing gaseous shell. Note that equation (4) is only valid in the bimodal parameter space, i.e. it can only be applied to clusters with a mechanical power that exceeds the threshold value  $L_{crit}$ , and carries a strong implicit dependence on  $\eta$  via the threshold mechanical luminosity,  $L_{crit}$  and the star cluster wind terminal speed,  $V_{\infty}$  (see Wünsch et al. 2007; Silich et al. 2007):

$$L_{crit} = \frac{3\pi\eta\alpha^2\mu_i^2 R_{SC} V_{A\infty}^4}{2\Lambda_{st}} \left( \frac{\eta V_{A\infty}^2}{2} - \frac{c_{st}^2}{\gamma - 1} \right), \quad (5)$$

$$V_{\infty} = [2/(\gamma - 1)]^{1/2} c_{st} \quad (6)$$

where  $\alpha = 0.28$  and  $\mu_i = 14m_H/11$  is the mean mass per ion.  $\Lambda_{st}$  and  $c_{st}$  are the values of the cooling function and the speed of sound at the stagnation point, both are functions of temperature at the stagnation radius,  $T_{st}$ , which strongly depends also on  $\eta$ . We obtain the value of  $T_{st}$  from the condition that the stagnation pressure reaches the maximum possible value and thus  $dP_{st}/dT_{st} = 0$  (Tenorio-Tagle et al. 2007):

$$\left( \frac{\eta V_{A\infty}^2}{2} - \frac{c_{st}^2}{\gamma - 1} \right) \left( 1 - \frac{T_{st}}{2\Lambda} \frac{d\Lambda}{dT_{st}} \right) - \frac{1}{2} \frac{c_{st}^2}{\gamma - 1} = 0. \quad (7)$$

Note that the calculated heating efficiency does not depend significantly on the parameter  $f_t$ . Hereafter we shall assume that  $f_t = 0.5$  and  $V_{A\infty} = 1000 \text{ km s}^{-1}$ .

In order to relate the star cluster mass with the star cluster mechanical luminosity we use a relation, which approximates the results of Starburst 99 synthesis model for coeval clusters with a Salpeter initial mass function with sources between  $1 M_{\odot}$  and  $100 M_{\odot}$  and ages in the range  $\sim 4$  Myr - 12 Myr (Leitherer et al. 1999):

$$L_{SC} = 3 \times 10^{40} \left( \frac{M_{SC}}{10^6 M_{\odot}} \right) \text{ erg s}^{-1}. \quad (8)$$

Equation (4) presents only a weak dependence on  $L_{SC}$  and thus deviations of the star cluster mechanical luminosity from the assumed constant value do not affect the final results significantly.

Thus, in this approach one can obtain the heating efficiency  $\eta$  directly from the observed parameters of the stellar cluster and its associated HII region:  $M_{SC}$ ,  $R_{SC}$ ,  $N^{SC}$ ,  $R_{HII}$  and  $n_{HII}$  by solving equation (4).

#### 4. A sample of clusters in M82

In order to learn how efficient the conversion of the star cluster mechanical luminosity into the wind driving energy is, one needs a sample of clusters whose masses, sizes and Lyman continuum radiation are known together with the radius and density of their adjacent HII regions. Most of these parameters can be obtained from the photometric sample of Melo et al. (2005) who cataloged 197 young super stellar clusters in the central zone of the galaxy M82. The only parameter, which is required by equation (4) and which Melo et al. (2005) did not obtain, is the density of the ionized gas in the HII regions. We obtain this quantity from *Potsdam Multi Aperture Spectrophotometer*, PMAS (Roth et al. 2005) observations at the 3.5 m telescope in Calar Alto. PMAS is a very versatile instrument, with several working modes. Here, we used its lens array (LARR) which is made out of  $16 \times 16$  square elements. We observed the nuclear region of M82 using two continuous fields with the spatial sampling of  $0''.5 \times 0''.5$  and thus, covering a field of view of  $8''.0 \times 8''.0$  per pointing. Two different sets of observations were provided. A set of data with low spectral resolution, covering the whole optical spectral range was obtained in service mode on the 3rd and 4th of June 2005 while that with a high spectral resolution on the 2nd of February 2005. Both sets of data were taken under non-photometric conditions. Seeing ranged typically between  $1''.3$  and  $1''.6$ . Line profiles were fitted using gaussian functions. This procedure was done in an automatic way using the IDL based routine MPFITEXPR implemented by Markwardt<sup>4</sup> checking each fit,

---

<sup>4</sup>See <http://cow.physics.wisc.edu/~craigm/idl/idl.html>.

afterwards. A single gaussian fit was enough in order to reproduce the observed profiles. For each set of lines, wavelength differences between them were fixed and the same line width was assumed. Then the intensity maps of  $H_\alpha$  and  $S_{II}$  lines were produced.

Our field of view includes region A (O’Connell & Mangano, 1978) of the central zone as well as a highly extinguished heart-shaped region towards the west. In order to localize the selected clusters in the PMAS map, the resolution of the HST image was degraded to  $0''.506$  / pixel, which is almost identical to that of PMAS ( $0''.5$  / pixel) and a new, low resolution HST  $H_\alpha$  map of M82 nuclear region was generated. As we did not have absolute astrometry and in order to use the two observing data sets, the low-resolution HST and the PMAS  $H_\alpha$  maps were compared and displaced until reaching the highest cross correlation coefficient (Russ, 2002). Then the electron density,  $n_{HII}$ , was derived (see Table 2) from a map of the  $[S\ II]\lambda 6717 / [S\ II]\lambda 6731$  line ratio using the task `temden`, based on the `fiwel` program (Shaw & Dufour, 1995), included in the IRAF package `nebular` and assuming an electronic temperature of 10000 K (see Figure 1).

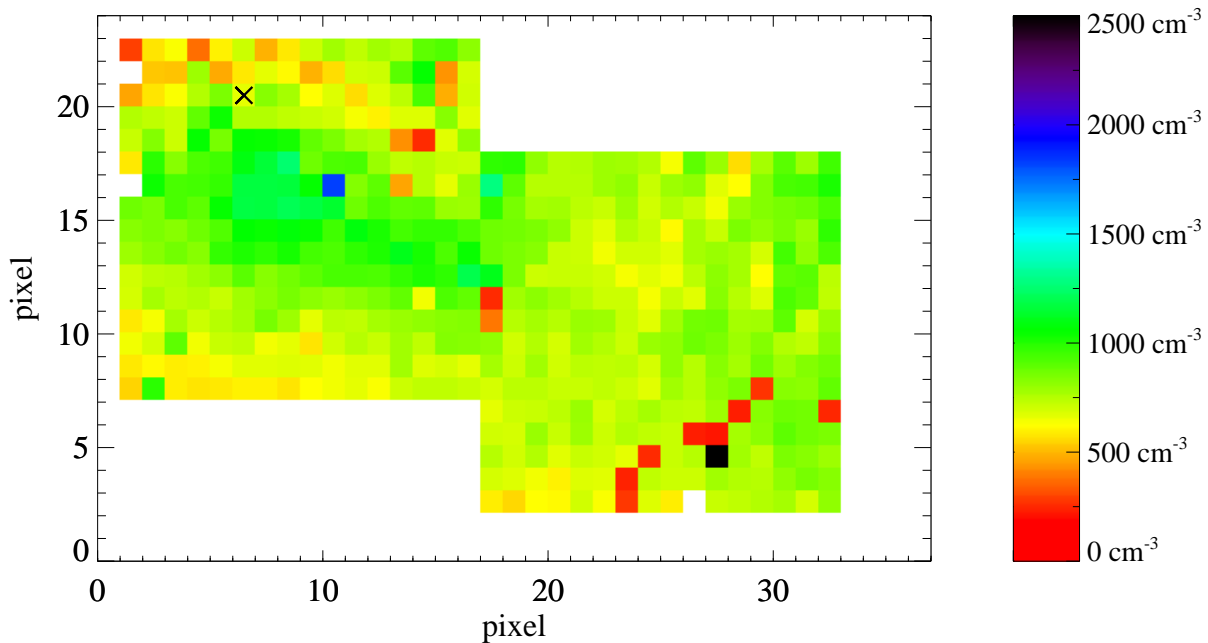


Fig. 1.— The ionized gas density distribution derived from the PMAS observations. The range of densities is coded by color scale on the right of the panel. Positions of different points in the field of view of PMAS are given in pixels. The position of the M82-A1 cluster is marked with a cross symbol.

We use the electron density values and the photoionization balance equation in order to estimate the masses of the associated HII regions:

$$M_{HII} = \frac{\mu_i N^{SC}}{\beta n_{HII}}, \quad (9)$$

where  $\mu_i$  is the mean mass per ion and  $\beta = 2.59 \times 10^{-13} \text{ cm}^{-3} \text{ s}^{-1}$  is the recombination coefficient to all but the ground level.

84 out of the 197 clusters found by Melo et al. (2005) are located in the area observed with PMAS. From the large sample of young SSCs cataloged by Melo et al. (2005) we have selected a subsample which follows the criteria that the radius of the HII region (the one defined in the  $H_\alpha$  HST images) lies clearly outside the volume occupied by the SSCs themselves (radius taken from the continuum HST images). In this way we selected a total of 21 objects. We then compared our list of cluster candidates with that of Mayya et al. (2008), who used the HST Advanced Camera for Surveys (ACS) and selected only those sources, which were simultaneously detected in three different (B, V and I) filters. Only 10 counterparts for our 21 candidate clusters were found in the list of Mayya et al. (2008). We have selected these as genuine clusters for our further discussion. Figure 2 presents the location of the selected clusters within the galaxy and also outlines the area in the central zone of M82, which was observed with PMAS.

Table 1 presents the identification of the selected clusters. Here the first column marks the clusters in our list, columns 2 and 3 provide the star cluster and the M82 zone identification in the sample of Melo et al. (2005) and column 4 lists the identification number in the sample of Mayya et al. (2008).

Table 2 presents the star cluster masses and radii (columns 2 and 3, respectively) and the number of Lyman continuum photons (column 4) taken from Melo et al. (2005). The number densities, radii and masses of the associated HII regions are given in columns 5, 6 and 7, respectively. Column 8 presents the calculated values of the heating efficiency and column 9 - the output mechanical luminosity normalized to the star cluster mechanical luminosity,  $L_{SC}$ , predicted by the Starburst 99 synthetic model.

Note that the cluster radii fall into a narrow size interval,  $2 < R_{SC} < 6$  pc whereas their masses vary from  $2 \times 10^4 M_\odot$  to  $8 \times 10^5 M_\odot$ . In all selected cases the resulting masses of the associated HII regions do not exceed a few thousand solar masses, just as in the case of M82-A1 whose stellar mass is  $\sim 10^6 M_\odot$  and its associated HII region has only  $\sim 5000 M_\odot$  (Smith et al. 2006).

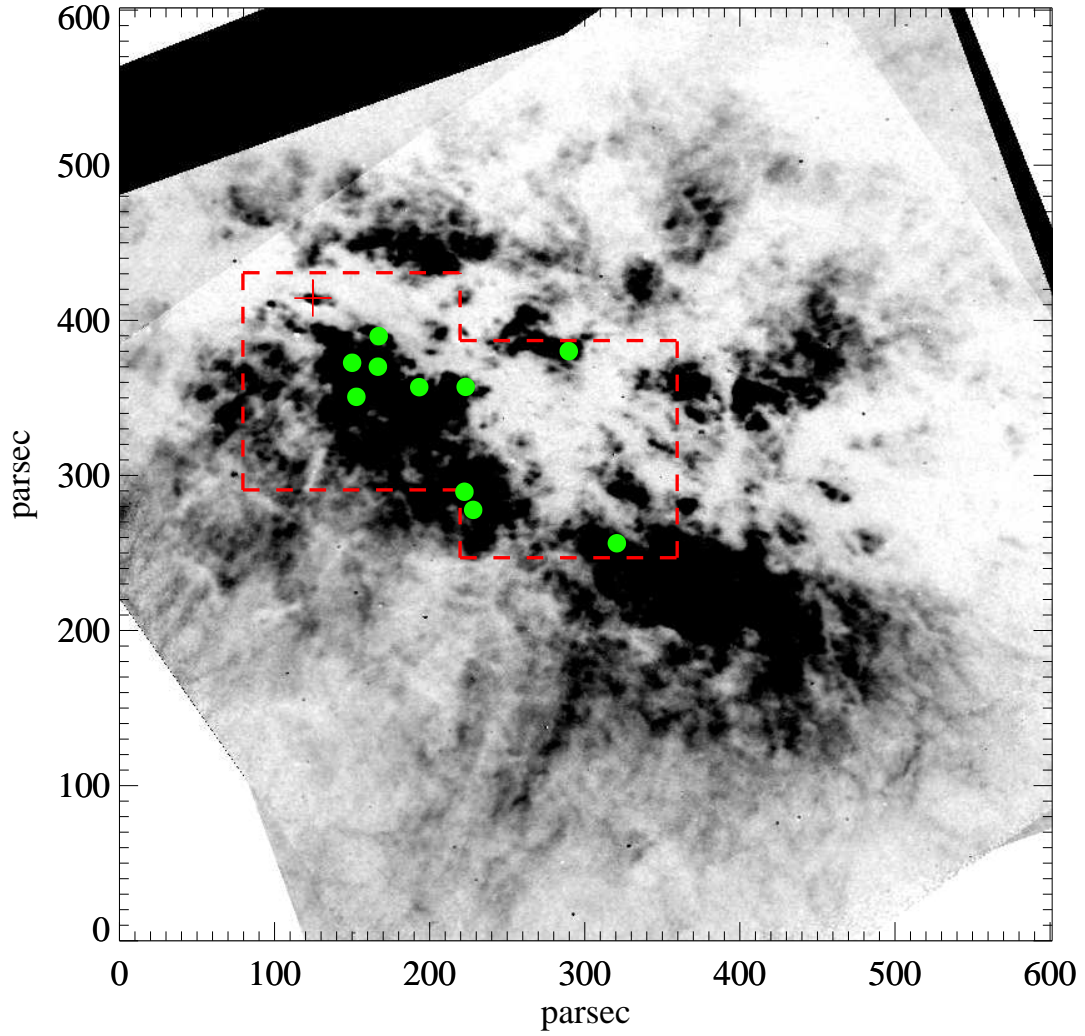


Fig. 2.— The HST WFPC2 image of the central zone of M82 taken in the F656N filter. The selected clusters are shown as green dots. The position of the M82-A1 cluster is used as a reference point and is marked with a red plus. Dashed lines outline the field of view of PMAS.

Table 1: Selected clusters

| Cluster | ID                 | zone | ID                  |
|---------|--------------------|------|---------------------|
|         | Melo et al. (2005) |      | Mayya et al. (2008) |
| (1)     | (2)                | (3)  | (4)                 |
| 1       | 20                 | SW   | 178N                |
| 2       | 52                 | SE   | 47N                 |
| 3       | 12                 | SE   | 13N                 |
| 4       | 58                 | SE   | 34N                 |
| 5       | 14                 | SE   | 20N                 |
| 6       | 59                 | SE   | 45N                 |
| 7       | 3                  | NE   | 71N                 |
| 8       | 72                 | SE   | 200N                |
| 9       | 81                 | SE   | 32N                 |
| 10      | 75                 | SE   | 28N                 |

Table 2: Parameters of the selected clusters and their HII regions

| Cluster | $M_{SC}$             | $R_{SC}$ | $N^{SC}$             | $n_{HII}$       | $R_{HII}$ | $M_{HII}$       | $\eta$          | $L_{out}/L_{SC}$  |
|---------|----------------------|----------|----------------------|-----------------|-----------|-----------------|-----------------|-------------------|
|         | ( $10^5 M_{\odot}$ ) | (pc)     | ( $10^{49} s^{-1}$ ) | ( $cm^{-3}$ )   | (pc)      | ( $M_{\odot}$ ) | %               | %                 |
| (1)     | (2)                  | (3)      | (4)                  | (5)             | (6)       | (7)             | (8)             | (9)               |
| 1       | $0.35^{\pm 0.16}$    | 4.03     | $7.1^{\pm 3.7}$      | $769^{\pm 76}$  | 5.64      | 381.6           | $7.8^{\pm 2.1}$ | $3.17^{\pm 1.06}$ |
| 2       | $0.40^{\pm 0.16}$    | 4.03     | $34.0^{\pm 21.0}$    | $950^{\pm 51}$  | 4.83      | 1479.3          | $7.0^{\pm 1.9}$ | $2.46^{\pm 0.93}$ |
| 3       | $1.25^{\pm 0.92}$    | 4.83     | $17.7^{\pm 9.4}$     | $706^{\pm 71}$  | 5.64      | 1036.2          | $5.0^{\pm 1.1}$ | $0.83^{\pm 0.34}$ |
| 4       | $0.64^{\pm 0.14}$    | 3.22     | $19.0^{\pm 7.9}$     | $953^{\pm 81}$  | 4.03      | 824.1           | $5.3^{\pm 1.2}$ | $1.04^{\pm 0.44}$ |
| 5       | $1.30^{\pm 1.0}$     | 3.22     | $15.2^{\pm 8.4}$     | $665^{\pm 60}$  | 5.64      | 944.8           | $5.2^{\pm 1.2}$ | $0.71^{\pm 0.31}$ |
| 6       | $4.00^{\pm 3.7}$     | 4.03     | $24.0^{\pm 12.0}$    | $886^{\pm 115}$ | 4.83      | 1119.6          | $4.0^{\pm 0.8}$ | $0.23^{\pm 0.12}$ |
| 7       | $2.19^{\pm 0.47}$    | 3.22     | $58.0^{\pm 22.0}$    | $771^{\pm 170}$ | 4.83      | 3109.4          | $4.3^{\pm 0.8}$ | $0.33^{\pm 0.15}$ |
| 8       | $1.45^{\pm 0.33}$    | 2.42     | $16.6^{\pm 5.1}$     | $1146^{\pm 76}$ | 3.22      | 598.7           | $4.3^{\pm 0.9}$ | $0.34^{\pm 0.18}$ |
| 9       | $3.60^{\pm 2.1}$     | 3.22     | $18.0^{\pm 8.2}$     | $850^{\pm 145}$ | 4.03      | 875.3           | $3.7^{\pm 0.6}$ | $0.17^{\pm 0.08}$ |
| 10      | $2.40^{\pm 2.2}$     | 2.42     | $24.0^{\pm 15.0}$    | $1163^{\pm 82}$ | 4.83      | 853.0           | $5.6^{\pm 1.7}$ | $0.53^{\pm 0.28}$ |

- Parameters of the clusters (columns 2, 3 and 4), radii of the associated HII regions (column 6) and uncertainties in their determination are taken from Melo et al. (2005).
- Ionized gas density (column 5) was derived from PMAS observations.
- One pixel uncertainty ( $\pm 0.81$  pc) was adopted in the determination of all radii.

### 5. Results and discussion

Each of the selected clusters (see Table 2) is surrounded by a compact HII region and has all attributes required by our model. We solve Equation (4) by iteration with the relative accuracy  $\Delta\eta/\eta \leq 10^{-5}$ . Equations (5), (6) and (7) were used every time when the iteration procedure requires new values for the threshold luminosity,  $L_{crit}$ , cooling function,  $\Lambda_{st}$ , and the star cluster wind terminal speed,  $V_\infty$ . Our results for each of the considered clusters are shown in Table 2 (column 9). We use the error propagation equation (Bevington & Robinson, 2003) in order to calculate the errors provided by the uncertainties in the determination of the input parameters of the model:  $M_{SC}$ ,  $R_{SC}$ ,  $N^{SC}$ ,  $R_{HII}$  and  $n_{HII}$ . Unfortunately, the uncertainties in the determination of the star cluster radii and sizes of the HII regions are not presented in the original paper of Melo et al. (2005). We take a 1 pixel ( $\pm 0.81$  pc) as a conservative estimate for the uncertainties in the measured radii.

The results of the calculations are presented in Figure 3, where the heating efficiency is presented as a function of star cluster radii and masses. It seems that there is a trend on panel b for the heating efficiency to be larger for less massive clusters. However this must be confirmed with better sets of input data. We also suggest for a future analysis that the star cluster stellar density may be a better input parameter, which combines the two major observables, the star cluster mass and radius, into a single parameter.

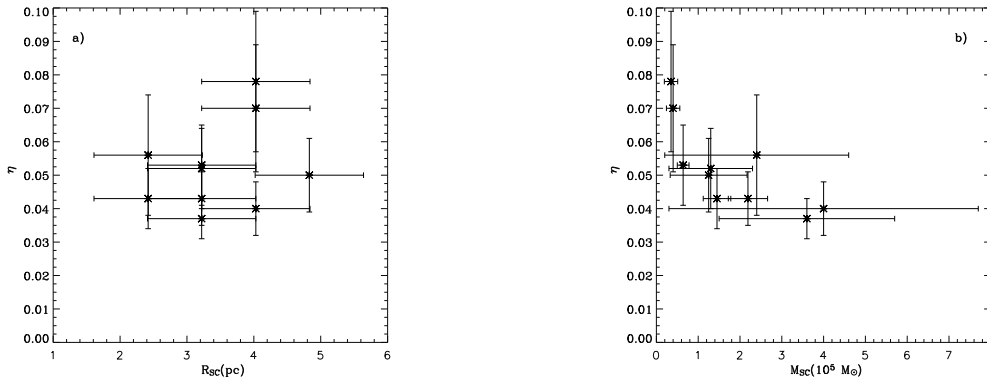


Fig. 3.— The calculated heating efficiency. Panels a and b present the star clusters heating efficiency as a function of star cluster radius and mass, respectively.

Figure 3 shows that the heating efficiency does not exceed 10% for all clusters in our sample. This implies that our massive and compact stellar clusters have a much reduced outflow velocity and negative feedback into the ambient ISM than what one would expect

using synthetic models. Indeed, the mechanical energy output rate is:

$$L_{out} = \frac{1}{2} \dot{M}_{out} V_{\infty}^2, \quad (10)$$

where the star cluster wind terminal speed,  $V_{\infty}$ , is defined by equations (7) and (6) and the mass output rate,  $\dot{M}_{out}$ , is (Wünsch et al. 2007):

$$\dot{M}_{out} = \dot{M}_{SC} \left( \frac{L_{crit}}{L_{SC}} \right)^{1/2}. \quad (11)$$

The critical luminosity,  $L_{crit}$ , is defined by equation (5). The fraction of the injected mechanical energy,  $L_{out}/L_{SC}$ , that a cluster returns to the ambient ISM thus is:

$$\frac{L_{out}}{L_{SC}} = \left( \frac{L_{crit}}{L_{SC}} \right)^{1/2} \left( \frac{V_{\infty}}{V_{A\infty}} \right)^2. \quad (12)$$

The calculated mechanical energy output does not exceed a few per cent of the star cluster mechanical luminosity for all selected clusters (see Table 2). Only in this way the shock-heated matter driven out as a cluster wind can cool rapidly to  $T \leq 10^4$  K and be photoionized while a high ambient pressure prevents its expansion into the surrounding interstellar medium.

The implication of our results, when compared with the recently inferred (Strickland & Heckman, 2009) net efficiency of supernova and stellar wind feedback in the nucleus of M82 ( $\geq 30\%$ ), is that there is a phase, a time during which massive and compact clusters have a low heating efficiency and undergo a bimodal hydrodynamic solution returning to the ISM of their host galaxy only a small fraction of mass and mechanical energy released inside the star cluster volume. Here we suggest that the selected young, massive clusters pass through such special phase in their hydrodynamical evolution, highlighted observationally by the presence of a compact HII region. Indeed, the relevant cluster parameters such as: the energy and mass deposition rates, the mean separation between nearby energy sources and the chemical composition of the injected matter - all change with time. This must lead to important changes in  $\eta$  and thus to large displacements of the threshold luminosity and noticeable changes in the rates of mass,  $\dot{M}_{out}$ , and energy,  $L_{out}$ , which a star cluster returns to the ISM. The time evolution of  $\eta$  will be the subject of a forthcoming communication.

We thank our anonymous referee for a critical review. We also appreciate fruitful discussions with Divakara Mayya and Daniel Rosa-González dealing with their selection criteria of stellar clusters in M82. This study has been supported by CONACYT - México, research grants 82912 and 60333, and partially funded by AYA2007-67965-CO3-O1 from the Spanish Consejo Superior de Investigaciones Científicas and the Spanish MEC under the Consolider-Ingenio 2010 Program grant CSD2006-00070: First Science with the GTC.

## REFERENCES

- Bevington, P. R. & Robinson, D. K. *Data Reduction and Error Analysis for the Physical Sciences*, 2003, The McGraw-Hill Companies, NY, p. 41
- Bisnovatyi-Kogan, G. S. & Silich, S. A. 1995, *Rev. Mod. Phys.* 67, 661
- Bradamante F., Matteucci, F. & D’Ercole, A. 1998, *A&A*, 337, 338
- Chevalier, R. A. & Clegg, A. W. 1985, *Nature*, 317, 44
- Chu, Y.-H., Chang, H.-W., Su, Y.-L. & Mac Low, M.-M. 1995, *ApJ*, 450, 157
- Cooper, J. L., Bicknell, G. V., Sutherland, R. S. & Bland-Hawthorn, J. 2008, *ApJ*, 674, 157
- Ehlerová, S., Palouš, J. & Wünsch, R. 2004, *ApSS*, 289, 279
- Hägele, G. F., Díaz, A. I., Cardaci, M. V., Terlevich, E. & Terlevich, R. 2007, *MNRAS*, 378, 163
- Leitherer, C., Schaerer, D., Goldader, J.D. et al., 1999, *ApJS*, 123, 3
- Lozinskaya, T. 1992, *Supernovae and stellar wind in the interstellar medium*, NY: American Institute of Physics
- Luo, D., McCray, R. & Mac Low, M.-M. 1990, *ApJ*, 362, 267
- Mac Low, M.-M. & McCray, R. 1988, *ApJ*, 324, 776
- Mayya, Y. D., Romano, R., Rodríguez-Merino, L. H., Luna, A., Carrasco, L. & Rosa-González, D. 2008, *ApJ*, 679, 404
- Meaburn, J. 1980, *MNRAS*, 192, 365
- Melo, V. P., Muñoz-Tuñón, C., Maíz-Apellániz, J. & Tenorio-Tagle, G. 2005, *ApJ*, 619, 270
- O’Connell, R. W. & Mangano, J. J. 1978, *ApJ*, 221, 62
- Puche, D., Westpfahl, D., Brinks, E. & Roy, J.-R. 1992, *AJ*, 103, 1841
- Recchi, S., Matteucci, F. & D’Ercole, A. 2001, *MNRAS*, 322, 800
- Roth, M. M., Kelz, A., Fechner, T. et al. 2005, *PASP*, 117, 620
- Russ, J. C. *The image processing handbook*, 2002, CRC Press, p.527

- Shaw, R. A., & Dufour, R. J. 1995, *PASP*, 107, 896
- Silich, S., Tenorio-Tagle G. & Añorve Zeferino, G.A. 2005, *ApJ*, 635, 1116
- Silich, S., Tenorio-Tagle, G. & Muñoz-Tuñón, C. 2007, *ApJ*, 669, 952
- Silich, S., Tenorio-Tagle G. & Rodríguez González, A. 2004, *ApJ*, 610, 226
- Smith, L.J., Westmoquette, M.S., Gallagher, J.S. III, O’Connell, R.W., Rosario, D.J. & de Grijs, R. 2006, *MNRAS*, 370, 513
- Stevens, I. R., Blondin, J. M. & Pollock, A. M. T. 1992, *ApJ*, 386, 265
- Stevens, I.R. & Hartwell, J.M. 2003, *MNRAS*, 339, 280
- Strickland, D. K. & Heckman, T. M. 2009, *astro-ph/0903.4175*
- Tenorio-Tagle, G., Muñoz-Tuñón, C., Pérez, E., Silich, S. & Telles, E. 2006, *ApJ*, 643, 186
- Tenorio-Tagle G., Silich, S. & Muñoz-Tuñón, C. 2003, *ApJ*, 597, 279
- Tenorio-Tagle, G., Silich, S., Rodríguez-González A. & Muñoz-Tuñón, C., 2005, *ApJ Lett.* 628, L13
- Tenorio-Tagle, G., Wunsch, R., Silich, S. & Palouš, J. 2007, *ApJ*, 658, 1196
- Weaver, R., McCray, R., Castor, J., Shapiro, P. & Moore, R. 1977, *ApJ*, 218, 377
- Wunsch, R., Silich, S. Palouš, J. & Tenorio-Tagle, G. 2007, *A&A*, 471, 579
- Wunsch, R., Tenorio-Tagle, G., Palouš, J. & Silich, S. 2008, *ApJ*, 683, 683